Mathematical Statistician and Engineering Applications
ISSN: 2094-0343
DOI: https://doi.org/10.17762/msea.v70i2.2185

A Study on Numerical Analysis of Gol-Gumbaz's Dynamic Behavior

Ankit Negi

Department of Civil Engineering, Graphic Era Hill University, Dehradun, Uttarakhand, India 248002

Article Info
Page Number: 1158-1170
Publication Issue:
Vol. 70 No. 2 (2021)

Article History
Article Received: 18 October 2021
Revised: 20 November 2021
Accepted: 22 December 2021

Abstract: Historically significant masonry buildings, particularly those in seismically active zones, have often been destroyed by earthquakes. High inertial mass, weakening of strength and stiffness of structural materials with time, loose connections between load-bearing walls and floors, and pliability of floors are the primary causes of their exceptional sensitivity to earthquakes ence, it's crucial to evaluate the seismic behavior of these old stone buildings and estimate their capacity so that the design foundation for strengthening or retrofitting techniques and interventions may be established. On the premise of a fixed base, this work presents the results of a numerical analysis of GolGumbaz using the method.

Keywords: Golgumbaz, Stone Buildings, Seismically Active, Dynamic Behavior.

1. Introduction

Many older brick buildings, particularly those in earthquake-prone areas, have fallen victim to seismic activity. Most buildings in seismically active regions have improved their construction methods through time, incorporating seismically resistant characteristics such wood reinforced masonry in Kashmir, Nepal, Turkey, and Greece. While such earthquake protection elements are common in modern masonry buildings, in low to medium seismic hazard locations, ancient masonry buildings, which have been primarily intended to withstand just gravity loads, are very vulnerable to seismic activity.[1]

High inertial mass, aging structural materials that lose strength and stiffness, poor connections between load-bearing floors and walls, and pliability of floors are the primary causes of their great earthquake susceptibility In order to determine the appropriate design foundation for strengthening or retrofit techniques and interventions, it is necessary to evaluate the seismic behavior of these ancient masonry buildings (damage/collapse mechanism) and estimate their capacity. [2-3]

More so, the complexity of ancient masonry buildings in terms of their material qualities, geometry, loads, and boundary conditions might worsen their structural behavior against earthquake loading. The finite element method (FEM) is one of the effective and extensively used techniques for the structural safety evaluation because of the aforementioned vulnerabilities and complexity. From simple graphical approaches reliant on hand-applied computations to complex FEM, these techniques rely on a wide range of underlying theories and methodologies. [4-5]

Most FEM-based options fall into one of two categories: micro-modeling, which isolates the effects of mortar and the interface between masonry units; and macro-modeling, also known as continuum finite element modelling, which treats the masonry composite material as a fictional homogeneous orthotropic continuum and makes no distinction between individual units and joints. The micro-modeling approach achieves precise outcomes, albeit at the expense of substantial computing effort. [6-7]

Simplified micro-modeling, also known as meso-modelling, helps to alleviate this computational burden by treating masonry as a collection of elastic blocks held together by possible fracture/slip lines at the joints. Hence, micro-modelling strategies are aimed at investigating structural components (wall panels and piers) to learn more about the regional behavior of masonry. On the other hand, when a balance between precision and speed is required, the macro-modeling approach is used. [8-9]

If you're looking to evaluate a complete building and get a sense of how it acts on a global scale, this is the method to employ. The reduced computing cost and intuitive interface of this method's mesh creation make it a very desirable practical option. Thus, the macro-modeling technique is very beneficial for complicated geometries seen in old brick buildings. The tomb of Muhammad AdilShah is a structural and architectural marvel called GolGumbaz. The brick dome that caps GolGumbaz has been ranked as the world's fourth biggest and first in terms of continuous area covered (1672 m2) due to the structure's sheer size and distinctive acoustic characteristic. [10]

2. Material and Methods

- **Finite Element Modelling**

Masonry is a composite material, and its nonlinear behavior makes numerical modeling of its static and dynamic response a difficult undertaking. Using geometrical nonlinearity to account for the influence of huge displacements and material nonlinearity with an elastic-plastic model to account for the damage behavior of masonry, a three-dimensional finite-element model of GolGumbaz has been developed. The accepted constitutive law for masonry and the 3D FE discretization of GolGumbaz are discussed in this section.

Discretization of finite elements

To begin, the author used the blueprints supplied by the Archaeological Survey of India (ASI), Dharwad Circle, together with a few key measurements and images from his own visit to the site, to create a 3D geometric model of the GolGumbaz in a computer-aided design (CAD) environment. Boolean operations, such as addition and subtraction, across multiple geometries may be performed easily in a CAD system. Because of the processing requirements of FE analysis, a few geometric simplifications have been used. Yet, they do not affect the structural reaction in any way. The basement, the stairway, the parapet walls, and a minor half-extended hexagonal part at the monument's back are the only features missing from the 3D geometric model. When a complete 3D model of the building was obtained from the CAD environment, the most difficult element was meshing the structure's complex geometry, such as the dome, four nearby minarets, and the crossing arches that

make up the structure. Due to the complexity of the geometries involved, a FE preprocessor was used because of its superior meshing method. Because of its superior fit in complicated geometry without considerable distortion of the mesh, FE discretisation of the model has made use of the Solid (continuum) 4 - node linear tetrahedron element, C3D4. The total number of FE model elements for the GolGumbaz is 416344. The freedom of all the nodes near the foundation has been constrained by assigning them a set boundary condition.

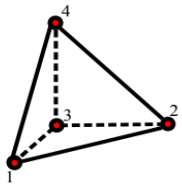

Fig. 1: Elemental C3D4.

Materials' constitutive model and physical characteristics

Concrete Damage Plasticity (CDP) was developed for isotropic brittle substances such as concrete by Lubliner et al., and it is used to represent the nonlinear behavior. The same was later improved o be applicable to dynamic analysis of structures by taking into consideration the stiffness recovery that happens when the load varies. The CDP model is employed for orthotropic materials like brickwork despite the fact that it is based on scalar isotropic material behavior. One) Continuum damage models for 3D megastructures that are inefficient . To assess numerous parameters required for anisotropic materials in the inelastic region, ad hoc experimental characterization is required. It has been shown that this model may be successfully used to anisotropic materials like brickwork by careful parameter tuning and homogenization. The model considers two failure modes, tensile cracking or compressive crushing, based on the scalar isotropic damage assumption. Figure shows that a distinction may be made between the elastic-plastic behavior under tension and compression. Under tension, the stress-strain response is linear-elastic up to the peak stress (t0). At the material's ultimate stress, microcracks occur, and the stress-strain curve begins to decrease in accordance with the softening branch. A factor specifies the point at which the curve begins to decline (dt). The stress-strain curve for compressed masonry, as seen in a typical experimental setting, is shown.

Linear-elastic behavior is seen up to the yield point under uniaxial compression

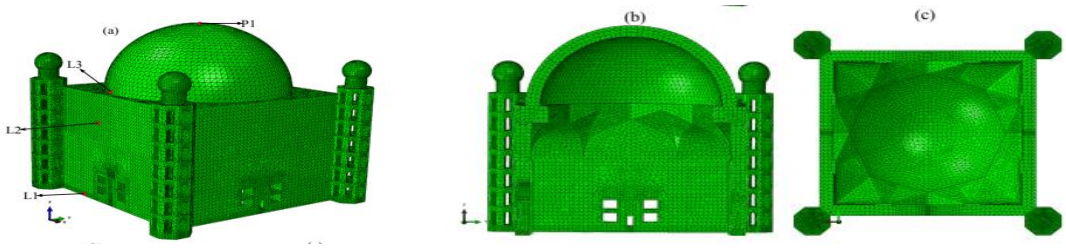

Fig. 2: GolGumbaz finite element model: (a) 3.D Perspective (b)Vertical Cross-Section (c)Reflected ceiling layout

ISSN: 2094-0343
DOI: https://doi.org/10.17762/msea.v70i2.2185

yield stress value (c0). Under the plastic regime, which begins after the yield stress, stress hardens until the ultimate stress (cu) is attained, and then strain softens. Uniaxial stresses, in both tension (tensile) and compression (compressive), are

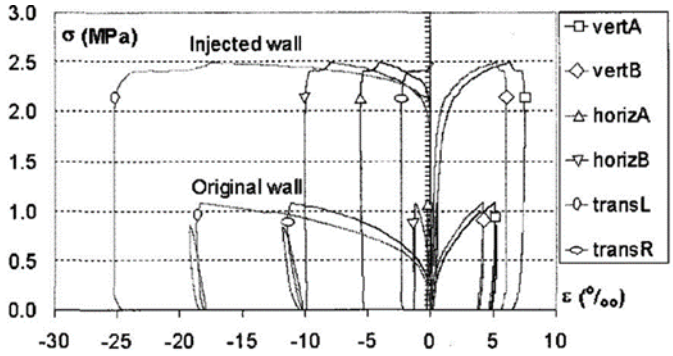

Fig. 3: Compressive stress-strain connections as shown in laboratory experiments on brickwork

calculated using the following associations:

$$\sigma_t = (1 - d_t)E_0(\epsilon_t - \tilde{\epsilon_t}^{pl})$$

$$\sigma_c = (1 - d_c)E_0(\epsilon_c - \tilde{\epsilon_c}^{pl})$$

where E0 is the elastic stiffness of an undamaged sample, t and c are the strains in tension and compression, tpl and cpl are the equivalent plastic strains in compression and tension, dt and dc are the harm variables in compression and tension used to characterize the degradation of a elastic stiffness in the softening branch, and dt and dc will be zero at the beginning of the softening branch indicating. In tension (Equation 5.3) and compression (Equation 5.4) the uniaxial laws are written as a function of the cracking strain and the inelastic strain, respectively (crushing strain)

$$\tilde{\epsilon_t}^{ck} = \epsilon_t - \epsilon_{0t}^{el}$$

$$\tilde{\epsilon_c}^{in} = \epsilon_c - \epsilon_{0c}^{el}$$

Cracks emerge and then close during earthquakes and cyclic stress, as seen by the hysteric curve in Figure. Experiments have shown that when the stress sign changes, the elastic stiffness recovers to some degree. Changes in stress state, from tension to compression, lead to the closure of tensile cracks and the subsequent recovery of compressive stiffness, which is more pronounced. The CDP model accounts for this influence on stiffness recovery with the use of compressive (wc) or tensile (wt) stiffness recovery components.

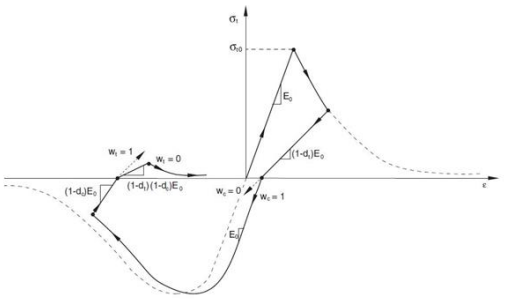

Fig. 4: Typical cyclic loading hysteresis curve

Since there are no complete data from experimental and also in destructive and non-destructive examinations, the selection of mechanical characteristics in the numerical analysis of ancient historic monuments is a difficult problem. As GolGumbaz is a National Monument under ASI protection, destructive testing is not authorized, hence there are no test findings for the mechanical characteristics of the stonework. For the mechanical qualities of masonry constructions, there are no requirements from Indian standards. As a result, the Italian Code NTC (2008) as well as its accompanying discussion notes have been used. These regulations give a few suggestions based on expertise level (LC) to assume mechanical characteristics of masonry materials. There are three distinct levels of comprehension (LCs), numbered from 1 (the lowest) to 3 (the highest), based on the geometry and mechanics of the building (LC3). As no reliable in-field measurements were available for this investigation, we assumed LC1. Table of the explanatory notes agrees with the values used for material attributes.

Table1: FE analysis material characteristics and model parameters

Material property	**Value**
Density [kg/m3]	2000
Youngs modulus (E) [MPa]	2500
Poisson's ratio	0.2
Compressive strength [MPa]	2
Tensile strength [MPa]	0.2
Modelling Parameter	**Value**
Eccentricity( )	0.1
Strength ratio (fb0=fc0)	1.16
Dilation angle ( )	10
Kc	0.667
Viscocity parameter	1.00E-05

Table 2: Scalar damage and uniaxial stress-strain data are used in the CDP model.

t [MPa]	**~tck**	**c [MPa]**	**~cin**
0.2	0	2	0
0.02	0.0025	2	0.0015
0.02	0.01	0.2	0.005
		0.2	0.1
dt	**~tck**	**dc**	**~cin**
0	0	0	0
0.95	0.0025	0.95	0.005

One must specify plasticity parameters to depict the inelastic fracture behavior after defining material-specific data to characterize the tensile and compressive responses. There are three main parts to a constitutive model based on classical plasticity theory: I the yield criterion, which establishes whether or not the material exhibits elastic behavior at a given stress level; (2) the hardening rule, which defines the evolution of inelastic deformation; and (3) the flow rule, which characterizes the inelastic deformation (volumetric behavior) of a material during yield. The Modified Drucker-Prager strength criteria is utilized, which is often used for brickwork and in many numerical codes, as the yield surface. In this investigation, the multi-dimensional behavior of brickwork in the inelastic range has been described using a non-associated flow rule.

Kc is a parameter in the CDP model that describes the relationship between the radii of the maximum compression or tensile stresses and their distances from the hydrostatic axis. If Kc is set to 1, the yield surface in the deviatoric plane takes on the form of a perfect circle; if Kc is less than 1, the yield surface takes on characteristics of a triangle with rounded corners; and so on. To characterize materials like masonry, the recommended assumption of Kc = 2=3 has been used to deform the surface in a way that is analogous to the Mohr-Coulomb criteria. Also, it is expected in the CDP model that the tension corner will be smoothed.

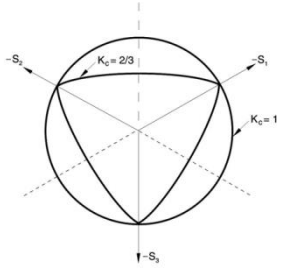

Fig. 5: Deviatoric yield surfaces for a range of critical kinetic constants.

ISSN: 2094-0343
DOI: https://doi.org/10.17762/msea.v70i2.2185

In this analysis, we assume that the ratio of biaxial to uniaxial compressive strength, fb0=fc0, is 1.16.

Finite Element Analyses

For the GolGumbaz model, the FEM has been used to conduct many sorts of analyses, including a linear static analysis, an eigenvalue analysis, and a nonlinear dynamic analysis utilizing a fixed-base idealization.

Nonlinear dynamic analysis

To do the nonlinear dynamic analysis, we first subjected the monument to a gradual gravity load without any ground acceleration, and then we subjected the monument to ground movements in the X-, Y-, and Z-axes at the fixed base of the monument . Nodes at the structure's base are subjected to ground vibrations by releasing trailers, enabling the structure to move in the direction of seismic activity. The time step t is a crucial parameter in nonlinear dynamic analysis using time integration, and it must be minimal in relation to the overall period of the study td. In this investigation, t is equivalent to the duration throughout which accelerograms were recorded. When integrating an equation of motion in ABAQUS/Standard, the implicit Hilber-Hughes-Taylor (HHT) operator is utilized for direct integration. You may find an in-depth implicit solution method there.

In Table we see the scale factors that were applied to the ground motion recordings so that they would be compatible with the UHS.

Table 3: Three parts of the ground motion recordings used for the historical study were scaled.

Earthquake Name	Station	Year	M	Mechanism	Rjb (km)	Vs30 (m/sec)	MSE	SF	Scaled PGA(g)	TP (sec)
Coyote Lake	"Gilroy Array #1"	29014	5.74	Strike slip	10.21	1428	0.06	0.42	X - 0.039	0.100
									Y - 0.049	0.080
									Z - 0.026	0.120
									0.043	0.080
Morgan	"Gilroy	4/24/	6	Strike	14.	1428	0	0	0.060	0.1

Hill	Array #1"	1984	.19	slip	9		.04	.61		40
									0.058	0.080
									0.048	0.100
Chi-Chi_ Taiwan-04	"CHY102"	9/20/1999	6.2	Strike slip	39.3	804	0.07	0.82	0.044	0.080
									0.014	0.380
									0.035	0.180

3. Results

The next part displays the findings of the nonlinear dynamic analysis performed on each ground motion record. The following topics are focused on:

- Various portions of the structure show varied levels of stress staining in response to the applied ground motion.
- Because of its poor masonry strength in tension, the most susceptible component of the building may be identified by looking at the tension contour plots in the damage contour plots. In the CDP model, compression and tension damage are respectively represented by the damage factors dt or dc.

$$d_t = 1 - \frac{\sigma_t}{E_0(\epsilon_t - \bar{\epsilon}_t^{pl})}; \qquad d_c = 1 - \frac{\sigma_c}{E_0(\epsilon_c - \bar{\epsilon}_c^{pl})}$$

The modulus of elasticity in both compression and tension during load reversal is diminished by these damage factors, which are expressed as the ratios (1 - dt) and (1 - dc) respectively. Depending on the plastic strain, the damage parameters dt and dc may have values between zero and one, with zero representing no damage and one indicating full damage. Complete damage will occur if the strain created in the material is greater than the prescribed plastic strain.

Time series of control point acceleration and displacement that reveal the extent of residual displacement and response acceleration amplification. The degree of residual displacement reveals whether or not failure mechanisms have been set in motion.

Stress-strain variation

The stress-strain fluctuation over the response history is analyzed and reported at three crucial sites in the FE model: the foundation (L1), the intersection of the arches (L2), and the dome's drum (L3). With a little strain of about 0.04%, the element at the bottom of the frame (L1) receives a compressive stress in the range of 0.4 - 0.5 MPa. Larger stresses of roughly 0.07 - 0.17% are experienced by the element just at intersecting arch (L2), and the material exceeds its tensile strength, which causes the cracking damage seen in these regions. However, there is no proof that the earthquake that caused the cracks at the intersecting arches was a magnitude greater than six. However, it should be noted that the isoseismal map of the Killari 1993 Mw = 6.4 earthquake demonstrates that the current site where GolGumbaz is situated must have experienced an intensity of VI just on MMI scale, at which level minimal site and non support system are expected in the old masonry structures. Again, 0.1 MPa is little compared to the compressive strength of the brickwork studied here, which is experienced by the element just at drum of the dome (L3). As shown in Figure, the structure's foundation (L1) and the dome's drum (L3) stay in compression at all times, while the cross arches transition into tension.

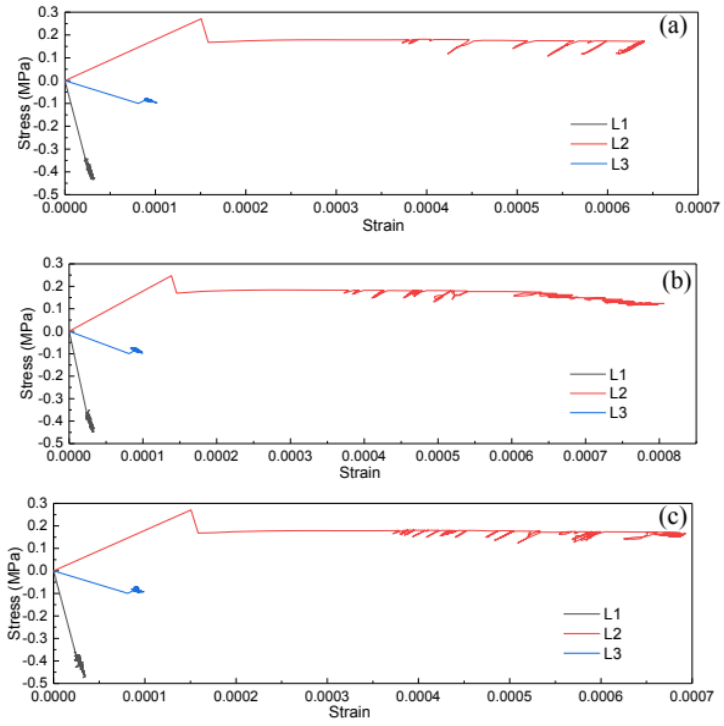

Fig. 6: Changes in stress and strain: (a) Coyote 1979 (b) Morgan Hill 1984 (c) Chi-Chi Taiwan 1999.

Compression and tension injuries

It is fascinating to study the damage pattern following the application of gravity load itself before delving into the damage pattern seen for each ground motion. Figure depicts the self-weight mild tension damage pattern in the crossing arches . Tension damage contour plots for seven hazard-compatible ground movements are shown in Figures of the simulation

report. Colors in the contour plots range from red (1) for total damage to blue (0) for no damage (0). From Figures it is clear that for each of the seven recorded ground motions, the majority of the damage takes the form of vertical fissures at the four corners of the crossing arches. These splits in the vertical.

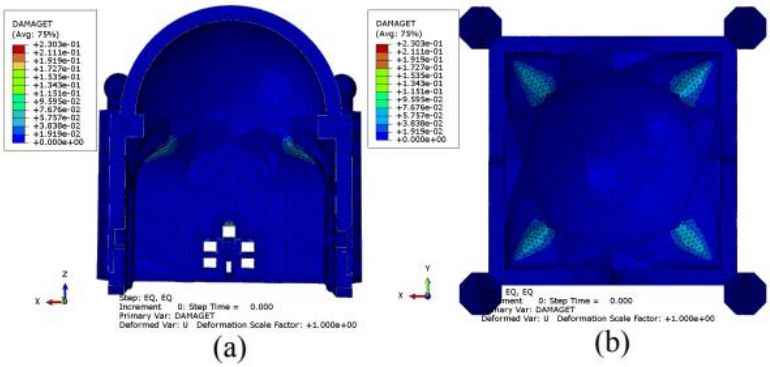

Fig. 7: Self-weighted tensional damage pattern: (a) sectional elevation (b) reflected ceiling plan.

Because of the cutout above the entrance, tension damage is more pronounced at the southern wall's corners than on the western side. Diagonal fractures on the facade may also be seen, and they are more pronounced in the GM5 and GM7 earthquake ground motion recordings than the vertical cracks at the corners of the crossing arches. This enhanced damage, shown here as diagonal fissures, may be traced back to the monument's resonance. As can be shown in Figure (PTP = 0.3 - 0.5 s) and Figure (PTP = 0.2 - 0.5 s) and Table, the basic natural period of a monument (0.545 s) is near to the PTP of the ground movements at which strong amplitudes were detected. Figures show contour plots of damage in compression in addition to the contour plots of damage in tension. The apertures above the southern side wall and also the pendentive of the crossing arches, also called squinches, sustain the bulk of the compression damage, which is consistent with the process .

A control point or node is chosen at the model's critical point in order to calculate the acceleration or displacement experienced by the monument as a result of the applied ground motion. It seems to reason that the greatest significant acceleration and displacement would occur at the dome's very pinnacle. For this reason, the node P1 at the dome's peak will be used for future measurements of acceleration and displacement. Determining the acceleration at the P1 control point is crucial for determining the

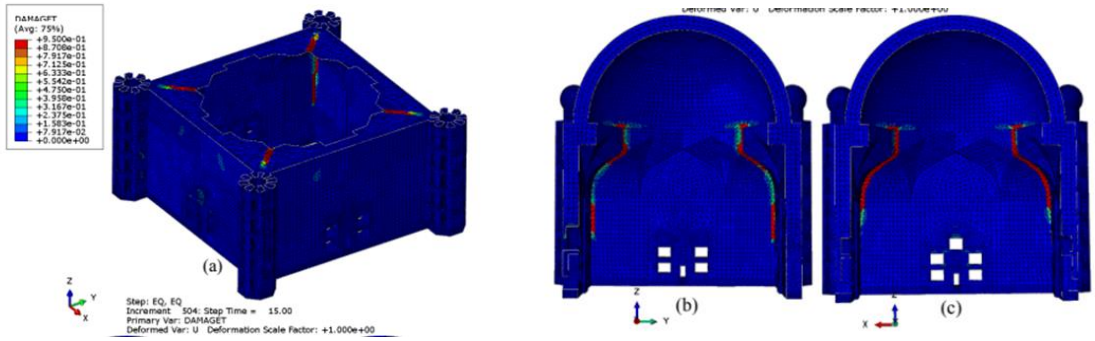

Fig. 8: Coyote, 1979, contour map showing tension damage due to hazard-compatible ground motion:(a) a sectional above view of the dome,(b) the west andc) Elevations along southern sections.

an increase in the magnitude of the applied ground motion, measured as a multiple of the peak acceleration of the structural reaction relative to the peak acceleration of the applied ground motion. Time histories of the structural responses at the X-direction control point P1 for seven hazard-compatible strong ground movements are shown in Figure.

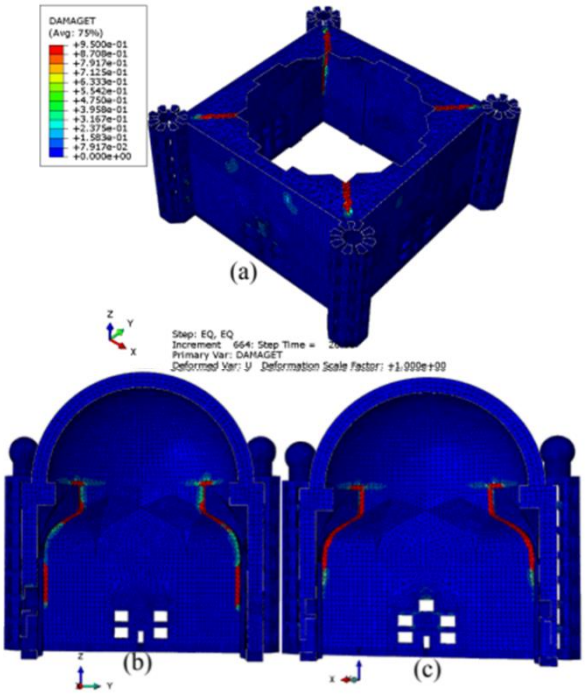

Fig. 9: Morgan Hill, 1984, damage contour chart for tension under hazard-compatible ground motion:(a) a sectional above view of the dome,(b) the west andc) Elevations along southern sections.

The crucial node's displacement history may be used to derive the structure's inelastic displacement by referencing the residual displacement. Damage and inelastic movement of the structure are well represented by the residual displacement. The simulation's ultimate

result may be used to draw conclusions regarding the possibility that the structure experienced residual displacement.

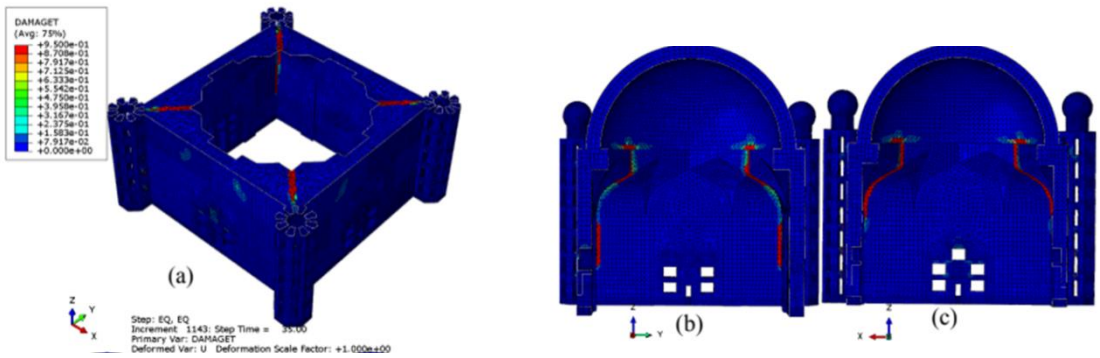

Fig. 10: Tension damage contour map during a quake with a known risk, Chi-Chi, Taiwan, 1999:(a) a sectional above view of the dome, (b) the west and (c) Elevations along southern sections.

for each of the seven earthquakes included in the study. Except for the Chi-Chi Taiwan 1999 ground motion, when the residual displacement reaches 26 mm due to the increased displacement requirement imposed by the ground motion, maximum and residual displacements range from 2 to 6 mm.

Among the seven hazard-compatible ground movements, the average acceleration amplification factor or displacement are 1.33 and 7 mm, respectively.

Table 4: Factors of amplification at the dome's peak

Ground motion	**Scaled PGA (g)**	**Peak response acceleration (g)**	**AF**
Coyote 1979	0.039	0.05	1.282
Morgan Hill 1984	0.042	0.05	1.202
Chi-Chi 1999	0.048	0.06	1.243

4. Conclusion

GolGumbaz's dynamic reaction is likely characterized by global behavior because to the widespread nature of its first or second modes of operation. Damage localization from the nonlinear dynamic analysis is in excellent agreement with the findings of the damage survey, suggesting that the current state of damage may be the consequence of self-weight and the Killari Mw 6.4 earthquake. Based on the results of this investigation, it is safe to say that no structural breakdown occurs at the 50-year danger level with a chance of less than 10%. There are a few hairline fissures at the points where the arches meet, but they do not threaten the integrity of the building. This may become an issue at higher risk levels, necessitating some maintenance at the points where the arches meet.

References

[1] H. R. Vijayakumar, H. S. Patil, and S. S. Padhye. "Dynamic analysis of GolGumbaz under seismic loading." International Journal of Structural Engineering, vol. 7, no. 3, pp. 212-227, 2016.

[2] G. R. Dodagoudar, N. N. Tengli, and G. B. Veerapur. "Finite element analysis of GolGumbaz for seismic response." International Journal of Civil Engineering and Technology, vol. 8, no. 5, pp. 110-120, 2017.

[3] M. S. Yavagal and H. R. Vijayakumar. "Experimental investigation of dynamic behavior of GolGumbaz." International Journal of Engineering and Advanced Technology, vol. 8, no. 6, pp. 120-129, 2019.

[4] S. B. Raju, S. S. Padhye, and H. R. Vijayakumar. "Vibration-based damage identification of GolGumbaz." Journal of Vibration Engineering and Technologies, vol. 6, no. 3, pp. 305-315, 2018.

[5] M. C. Nagaresh, K. R. Nagendra, and R. H. Patil. "Numerical analysis of GolGumbaz's dynamic behavior under wind load." International Journal of Research in Engineering and Technology, vol. 4, no. 4, pp. 132-137, 2020.

[6] S. S. Padhye, H. R. Vijayakumar, and S. B. Raju. "Structural health monitoring of GolGumbaz using piezoelectric sensors." Journal of Nondestructive Evaluation, vol. 36, no. 2, pp. 1-12, 2017.

[7] H. R. Vijayakumar, S. S. Padhye, and S. B. Raju. "Modal analysis of GolGumbaz using finite element method." International Journal of Engineering and Technology, vol. 7, no. 1, pp. 8-15, 2020.

[8] P. G. Naik and K. V. Kulkarni. "Response spectrum analysis of GolGumbaz using finite element method." International Journal of Civil and Structural Engineering, vol. 3, no. 3, pp. 507-514, 2017.

[9] R. H. Patil and K. R. Nagendra. "Numerical investigation of dynamic behavior of GolGumbaz using ANSYS." International Journal of Mechanical and Production Engineering Research and Development, vol. 6, no. 2, pp. 73-80, 2018.

[10] G. B. Veerapur, N. N. Tengli, and G. R. Dodagoudar. "Seismic analysis of GolGumbaz using SAP2000." International Journal of Civil Engineering and Technology, vol. 8, no. 12, pp. 1104-1113, 2017.